

Video Article

Facile Preparation of Internally Self-assembled Lipid Particles Stabilized by Carbon Nanotubes

Yogita Patil-Sen¹, Amin Sadeghpour², Michael Rappolt², Chandrashekhar V. Kulkarni¹

¹Centre for Materials Science, School of Physical Sciences and Computing, University of Central Lancashire

²School of Food Science & Nutrition, University of Leeds

Correspondence to: Chandrashekhar V. Kulkarni at cvkulkarni@uclan.ac.uk

URL: <https://www.jove.com/video/53489>

DOI: [doi:10.3791/53489](https://doi.org/10.3791/53489)

Keywords: Chemistry, Issue 108, carbon nanotubes, lipid nanostructures, lipid self-assembly, nanostructured lipid particles, Pickering emulsion, O/W emulsion, hybrid systems, biocompatibility, drug delivery, nanocarriers, coating carbon nanotubes

Date Published: 2/19/2016

Citation: Patil-Sen, Y., Sadeghpour, A., Rappolt, M., Kulkarni, C.V. Facile Preparation of Internally Self-assembled Lipid Particles Stabilized by Carbon Nanotubes. *J. Vis. Exp.* (108), e53489, doi:10.3791/53489 (2016).

Abstract

We present a facile method to prepare nanostructured lipid particles stabilized by carbon nanotubes (CNTs). Single-walled (pristine) and multi-walled (functionalized) CNTs are used as stabilizers to produce Pickering type oil-in-water (O/W) emulsions. Lipids namely, Dimodan U and Phytantriol are used as emulsifiers, which in excess water self-assemble into the bicontinuous cubic *Pn3m* phase. This highly viscous phase is fragmented into smaller particles using a probe ultrasonicator in presence of conventional surfactant stabilizers or CNTs as done here. Initially, the CNTs (powder form) are dispersed in water followed by further ultrasonication with the molten lipid to form the final emulsion. During this process the CNTs get coated with lipid molecules, which in turn are presumed to surround the lipid droplets to form a particulate emulsion that is stable for months. The average size of CNT-stabilized nanostructured lipid particles is in the submicron range, which compares well with the particles stabilized using conventional surfactants. Small angle X-ray scattering data confirms the retention of the original *Pn3m* cubic phase in the CNT-stabilized lipid dispersions as compared to the pure lipid phase (bulk state). Blue shift and lowering of the intensities in characteristic G and G' bands of CNTs observed in Raman spectroscopy characterize the interaction between CNT surface and lipid molecules. These results suggest that the interactions between the CNTs and lipids are responsible for their mutual stabilization in aqueous solutions. As the concentrations of CNTs employed for stabilization are very low and lipid molecules are able to functionalize the CNTs, the toxicity of CNTs is expected to be insignificant while their biocompatibility is greatly enhanced. Hence the present approach finds a great potential in various biomedical applications, for instance, for developing hybrid nanocarrier systems for the delivery of multiple functional molecules as in combination therapy or polytherapy.

Video Link

The video component of this article can be found at <https://www.jove.com/video/53489/>

Introduction

Over the last few decades, nanotechnology has emerged as a powerful tool especially in the field of preclinical development of medicine to combat notorious diseases such as cancer¹. In this context, nanoscale structures with size <1,000 nm are extensively explored as delivery vehicle of various active biomolecules such as drugs, proteins, nucleic acids, genes and diagnostic imaging agents¹⁻⁴. These biomolecules are either encapsulated within the nanoparticles or conjugated onto the surface of nanoparticles and are released at the site of action by triggers such as pH or temperature^{5,6}. Although extremely small in size, the large surface area of these nanoparticles proves to be greatly advantageous for targeted delivery of active biomolecules. The control over the particle size and biocompatibility is of utmost importance in order to optimize the therapeutic efficacy and hence the applicability of nanoparticles^{7,8}. Lipids⁹⁻¹³, polymers^{14,15}, metals^{16,17} and carbon nanotubes^{18,19} have been commonly employed as nanocarriers for various biomedical and pharmaceutical applications.

Moreover, nanocarrier applications based on lipid self-assembled nanostructures have a wide significance in many other disciplines including food and cosmetic industries^{20,21}. For instance, they are used in protein crystallization²², separation of biomolecules²³, as food stabilizers e.g., in desserts²⁴, and in the delivery of active molecules such as nutrients, flavors and perfumes²⁵⁻³¹. Self-assembled lipid nanostructures not only have the ability to release bioactive molecules in a controlled and targeted fashion³²⁻³⁸ but they are also able to protect the functional molecules from chemical and enzymatic degradation^{39,40}. Although planar fluid bilayer is the most common nanostructure formed by amphiphilic lipid molecules in presence of water, other structures such as hexagonal and cubic are also commonly observed^{20,41,42}. The type of nanostructure formed depend upon the lipids' molecular shape structure, the lipid composition in water as well as on the physico-chemical conditions employed such as temperature and pressure⁴³. The applicability of non-planar lipid nanostructures especially that of cubic phases, is restricted because of their high viscosity and non-homogeneous domain consistency. These problems are overcome by dispersing the lipid nanostructures in large amount of water to form oil-in-water (O/W) emulsions containing micron or submicron sized lipid particles. In this manner, a suitable product of low viscosity can be prepared while retaining the original lipid self-assembled structure inside the dispersed particles. The formation of these internally self-assembled particles (abbreviated as ISAsomes⁴⁴ e.g., cubosomes from cubic phases and hexosomes from hexagonal phases) commonly requires a combination of an high energy input step and the addition of stabilizers such as surfactants or polymers. Recent research

in this direction demonstrates the application of various solid particles⁴⁵ including silica nanoparticles⁴⁶, clay⁴⁷⁻⁴⁹ and carbon nanotubes⁵⁰ for the stabilization of aforementioned emulsions, suitably termed as Pickering⁵¹ or Ramsden-Pickering emulsions⁵².

In recent years, carbon based nanostructures such as single-walled carbon nanotubes (SWCNTs), multi-walled carbon nanotubes (MWCNTs) and fullerenes have received a great deal of attention as novel biomaterials^{53,54}. The main concerns are their toxicity⁵⁵⁻⁵⁸, water insolubility⁵⁹ and hence their biocompatibility⁵⁶. An efficient way to tackle these issues is the surface functionalization using non-toxic and biocompatible molecules such as lipids. In presence of water, lipids interact with CNTs in a manner that hydrophobic surface of CNTs is shielded from polar aqueous medium whereas the lipid hydrophilic head groups aid their solubility or dispersion in water^{60,61}. Lipids are integral constituents of cellular organelles as well as some food materials, therefore their decoration should ideally decrease the *in vivo* toxicity of CNTs. Biomedical applications based independently on CNTs^{18,19} and lipid nanostructures⁹⁻¹³ are under extensive development but the applications that combine properties of the two are not yet well-explored.

In this work, we employ two different types of lipids and three types of CNTs of which SWCNTs are in the pristine form whereas MWCNTs are functionalized with hydroxyl and carboxylic groups. We have used very low concentrations of CNTs to prepare the dispersions whose stability depends upon several factors e.g., the type of lipid, type of CNT, ratio of lipid to CNT used, as well as on the sonication parameters employed such as power and duration. This video protocol provides technical details of a method of kinetically stabilizing lipid nanoparticles using various CNT-stabilizers.

Protocol

Caution: CNTs used in this work are in the nanoparticulate form which may have additional hazards compared to their bulk counterparts. Inhalation of graphite, both natural and synthetic, can cause pneumoconiosis⁶² similar to coal worker's pneumoconiosis. Moreover, there have been concerns relating to the toxicity of carbon based nanostructures and some of the previous studies suggest acute and chronic toxicity associated with the inhalation of CNTs⁶³⁻⁶⁸. Hence, avoid inhalation of the fine CNT powder and handle it with great care. If inhaled, move to fresh air. If breathing is difficult, use pure oxygen instead and seek medical consultation. Solution/dispersion formulations of CNTs are rather safe to handle.

Caution: Lipids and surfactants used in this study are food-grade materials and thus non-hazardous in general, but they are irritant to eyes and skin, and also highly flammable. Hence, please use all appropriate safety practices such as use of engineering controls (fume hood) and personal protective equipment (safety glasses, gloves, lab coat, full length pants, closed-toe shoes) when handling or preparing nanoparticle samples. In case of contact with skin or eyes, immediately flush skin or eyes with plenty of water for at least 15 min. Seek medical advice if required.

1. Preparation of Lipid/Water Bulk Phases

Caution: Store the lipids in the refrigerator at 4 °C. Pure grade lipids should be stored in the freezer (-20 °C). Aliquot them into small glass vials to avoid contamination of the whole stock and convenience of handling. Other chemicals including CNTs and surfactants can be stored at RT but keep them away from direct sunlight.

1. Keep lipids, *i.e.*, Dimodan U (DU) and Phytantriol (PT) at RT for 15-20 min prior to opening the bottle/vial lid in order to avoid moisture condensation.
(Note: DU is a distilled glyceride comprising 96% monoglycerides and the rest are diglycerides and free fatty acids. Two major monoglyceride components in DU are linoleate (62%) and oleate (25%). Hence the hydrophobic part of DU mainly contains C18 chains (91%), the exact composition of which is as follows; C18:2 (61.9%), C18:1 (24.9%), and C18:0 (4.2%), where C18 indicates 18C-chain and the number after colon indicates number of C=C bonds. PT is a mixture of 3,7,11,15-tetramethyl-1,2,3-hexadecanetriol optical isomers. It does not contain an ester functional group but consists of highly branched phytanyl tail with a tri-hydroxy headgroup. Both of DU and PT form cubic phases in presence of excess water which is also the case for the cores of stabilized lipid particles^{13,45}).
2. Melt the lipids by putting vials in a hot water bath or a beaker containing water maintained above 60 °C (heating magnetic stirrer: 230 V, 50 Hz, 630 W or similar to be used to heat the water in a beaker).
3. Alternatively heat vials using block heaters. Do not heat the lipid containing vials directly on the hot plate in order to avoid temperature gradient and subsequent lipid decomposition.
4. Weigh 500 mg of the molten lipid, in previously weighed microcentrifuge tube (with conical snap cap, 1.5 ml), using a Pasteur glass pipette with a latex bulb.
5. Add 500 µl of ultrapure water (water resistivity=18.2 MΩ·cm) to the above microcentrifuge tube.
6. Mix the components manually for 15 min using tiny (custom-built) spatula. Make such a spatula by flattening the sharp end of a syringe needle (0.9 mm x 40 mm cannula length) using a plier.
7. Centrifuge the lipid/water mixture for 10 min at a speed of 2,000 x g. Again stir the mixture manually for 10 min, then equilibrate it for 24 hr. Before characterizing the samples, stir them for 5 min and then leave them at RT.
8. To ensure the formation of an equilibrium lipid phase throughout the entire tube, perform about 10 freeze-thaw cycles and intermittently carry out a centrifugation step as defined above. Both the DU and PT form highly viscous bulk lipid phases making it difficult to handle them manually (**Figure 1**).

Note: The above protocol (section 1) is only necessary, if one would like to compare nanostructural behavior (lattice type and dimensions of self-assembly) of dispersed particles with the bulk lipid phase and/or use it as a control to confirm the retention of original nanostructure.

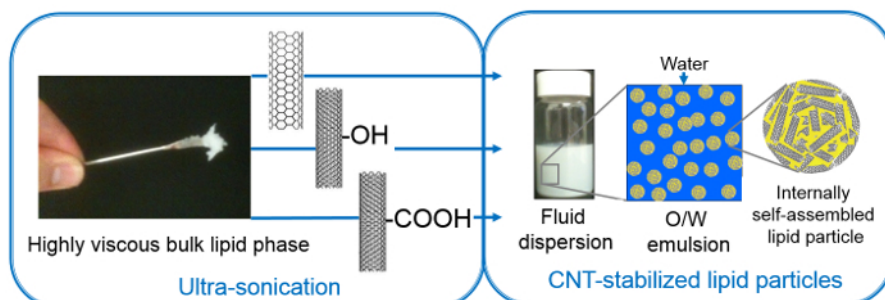


Figure 1. Preparation of O/W particulate emulsion with fluid consistency from highly viscous lipid phase using high energy input (ultrasonication) and using different CNT-stabilizers, namely SWCNT, MWCNT-OH, MWCNT-COOH (figure reproduced from reference [50] with permission from The Royal Society of Chemistry). Please click [here](#) to view a larger version of this figure.

2. Preparation of Surfactant Stabilized Lipid Particles

1. Prepare a 0.2% (w/w) surfactant (pluronic F127) solution in water.
 1. Dissolve 200 mg of the surfactant (white fluffy powder) in 100 ml ultrapure water by stirring it for 20-30 min (on a magnetic plate using a magnetic stirrer bar). Pluronic F127 is a non-ionic surfactant and is commonly used as emulsion stabilizer. It is a triblock copolymer of PEO₉₉-PPO₆₇-PEO₉₉, and hence takes long time to dissolve in water.
2. Add 500 mg of molten DU or PT (using a Pasteur glass pipette) to a glass vial (scintillation soda-lime fitted with foil lined urea cap, 20 ml).
3. Add 9.5 g of the 0.2% F127 solution.
4. On the probe ultrasonication machine, tightly clamp the vial to the retort stand jaw (Retort Stand Set with stand, clamp, base, rod, rubber 3 jaw and bosshead), so that it can withstand the vibrations generated by sonication.
5. Insert the solid titanium alloy probe (13 mm diameter x 139 mm length) attached to the Cell Sonicator. Adjust the height and position of the vial to ensure that its sides and bottom are not touching to the probe. A distance of 0.5 cm between the probe tip and the bottom of the glass vial gives good results.
6. Sonicate the mixture for 10 min in a pulsed mode with 1 sec pulse mediated by 1 sec delay time at 35% (of the maximum) power. The vial becomes very hot due to the heat generated during sonication. Therefore, allow it to cool down to RT before taking it off the clamp.
7. Store the milky-formed dispersion at RT for at least 24 hr, prior to further use. This is to ensure its stability against phase separation.

Note: Before and after using the probe, clean it with acetone, dry with a paper towel, then rinse it with ultrapure water and dry it once more.

3. Preparation of Dispersions of Pure CNTs in Water

1. In two separate beakers, weigh in 4 mg powdered MWCNT-OH and MWCNT-COOH, both of which are black in color.
2. Add 500 ml ultrapure water to each beaker. Using a probe ultrasonicator sonicate the mixtures for 2 min in a continuous pulse mode at 40% (of the maximum) power. The resulting concentration of the MWCNT dispersion is 8 µg/ml (stock solution).
3. Dilute the MWCNT stock solution with appropriate amounts of ultrapure water to achieve 6.25, 5, 4, 2 µg/ml MWCNT dispersions.
4. Sonicate these dispersions as described before (see 3.2).
5. Similarly, disperse 3 mg of powdered SWCNT (also black in color) in 500 ml ultrapure water to make a 6 µg/ml SWCNT dispersion (stock solution).
6. Dilute the SWCNT stock solution and sonicate them as described above (see 3.2) to obtain 0.5, 0.4, 0.3125, 0.2 µg/ml SWCNT dispersions.

Note: All dispersions are clear for about 30 min, after which the CNTs start to settle at the bottom.

4. Preparation of CNT-stabilized Nanostructured Lipid Particles (Figure 1)

1. Weigh in 500 mg of the molten DU into a glass vial.
2. Add 9.5 ml of the 6 µg/ml SWCNT dispersion to the vial.
3. Sonicate the CNT-DU mixture using the same parameters as used for making pure CNT dispersions (see 3.2). Upon cooling to RT, the CNT-stabilized lipid particles with conserved internally self-assembled nanostructure will be ready.
4. In a similar way, prepare the lipid particles using the 0.4 µg/ml and 0.2 µg/ml SWCNT dispersions.
5. Follow the protocols 4.1 to 4.4 to make lipid particles using MWCNT-OH and MWCNT-COOH but using different concentrations, namely 8, 4 and 2 µg/ml of CNT.
6. Similarly, prepare three different CNT-PT dispersions using 4 µg/ml MWCNT-OH and MWCNT-COOH as well as 0.4 µg/ml SWCNT. Note that the CNT-PT dispersions require less power (35% of the maximum) but longer time (15 min) in a continuous pulse mode. Cool the dispersions to RT and leave them for 24 hr before characterizing them.

Note: Sonication parameters may differ for different lipids (as for DU and PT here) and for different compositions; they need to be optimized to achieve well-stabilized dispersions.

5. Monitoring the Stability of the CNT-stabilized Lipid Dispersions

1. Monitor the stability of the dispersions by visual observation: check if the dispersions are destabilized or if lumps have formed in the dispersions.

- Take photos (with digital camera) at regular intervals. For instance, take pictures of dispersions every day in the first week, then every other day for a week followed by once a week for the next two weeks, and finally once a month as per requirement.

Representative Results

The following results represent a) the stability of dispersions, b) the size distribution of lipid particles, c) the type of self-assembly and d) the evidence for lipid coating of the CNTs. The stability of dispersions (**Figure 2**) was monitored using a 5 MP camera with auto-focus and LED flash.

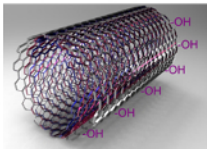



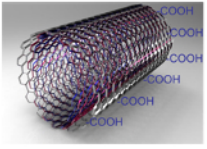



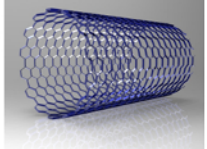



	CNT Type	Too little CNTs	Optimal CNT:Lipid Ratio	Excess CNTs
a)	 MWCNT-OH			
b)	 MWCNT-COOH			
	Conc.(μg/ml)	2.0	4.0	8.0
c)	 Pristine SWCNT			
	Conc.(μg/ml)	0.2	0.4	6.0

Figure 2. Schematics of CNT types (A) MWCNT-OH, (B) MWCNT-COOH, and (C) SWCNT and pictures of the corresponding emulsions. Stable emulsions were obtained only in a certain region (shaded) where the CNT to lipid ratio was optimum; below and above stable emulsion did not form because of a too little or too great amount of CNTs, respectively. An arrow indicates a typical CNT lump in an unstable emulsion. These measurements were performed for a range of DU-CNT dispersions; representative ones are shown here (figure reproduced from reference [50] with permission from The Royal Society of Chemistry). [Please click here to view a larger version of this figure.](#)

Small angle X-ray scattering (SAXS) patterns were recorded in order to determine the lattice type of the inner nanostructure of the stabilized isasomes (**Figure 3A**). The SAXSpace camera is connected to an analytical X-ray generating equipment (ISO-DEBYEFLEX3003) with a sealed-tube Cu-anode operating at 40 kV and 50 mA. The X-ray tube is chilled with a closed water circuit. The SAXSpace collimation block unit transforms the divergent polychromatic X-ray beam into a vertically focused line shaped beam of Cu-K α radiation with a wavelength, λ , of 0.154 nm. For the SAXS experiments the high resolution mode was chosen, which permits to detect a minimum scattering vector, q_{min} , of 0.04 nm $^{-1}$ ($q = (4\pi/\lambda) \sin\theta$, where 2θ is the scattering angle). A semi-transparent beam stop enables to record the attenuated primary beam profile for the exact determination of the zero scattering vector and transmission correction. Each of the studied samples is enclosed in the same vacuum-tight, reusable 1 mm quartz capillary to guarantee exactly the same scattering volume. The capillary was placed in the temperature controlled sample stage equipped with Peltier elements, which is connected to a water cooling thermostat to get rid of the excess heat. All experiments were performed at 25 °C with a temperature stability of 0.1 °C. A vacuum pump was used to evacuate the sample chamber achieving a minimum pressure of ~1 mbar. The 1D scattering patterns were recorded with a micro-strip X-ray detector. This detector is single photon counting and has a sensitive area of 64×8 mm 2 comprising 1,280 channels each with a channel size of 0.05 × 8 mm (v × h). The sample-detector distance was 317.09 mm. Each sample was exposed three times for 300 sec, and their integrated scattering profiles were averaged.

The SAXStreat software was employed to correct the scattering patterns with respect to the position of the primary beam. The SAXS data was further transmission-corrected by setting the attenuated scattering intensity at $q = 0$ to unity and the background was subtracted using the SAXSQuant software. The scattering vector q was calibrated with silver-behenate, which has a known lattice spacing of 5.84 nm $^{-1}$. All recorded diffraction patterns could be indexed with the space group $Pn3m$ (diamond bicontinuous cubic phase), in which the 110, 111, 200, 211, 220 and 221 reflections were identified (**Figure 3A**). The lattice parameter, a , for $Pn3m$ phase was determined by linear regression applying the following lattice equation

$$a = 2\pi/q_{hkl} \times \sqrt{h^2 + k^2 + l^2} \quad (1)$$

where h , k and l are the Miller indices.

The size and size distribution of dispersed lipid particles (**Figure 3B**) were determined using a laser particle size analyzer.

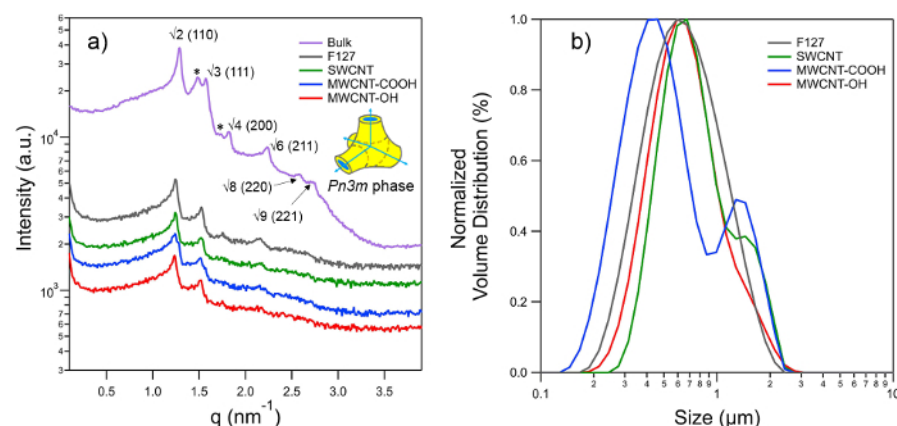


Figure 3. (A) SAXS patterns of the $Pn3m$ phase observed for bulk phytantriol (PT) and corresponding dispersions prepared with 5 wt% PT in excess water using F127 and different CNT stabilizers. The 3-D schematic diagram shown on the right displays part of the unit cell of $Pn3m$ phase, which is a bicontinuous cubic phase whose structure is based on double diamond (D) type minimal surface. Blue arrows indicate aqueous channels meeting at tetrahedral angle whereas hydrophobic and aqueous regions are color coded yellow and blue, respectively. Characteristic peaks for $Pn3m$ phase are indexed as $\sqrt{2}$, $\sqrt{3}$, $\sqrt{4}$, $\sqrt{6}$, $\sqrt{8}$, $\sqrt{9}$ and corresponding Miller indices are shown in the brackets. All of the above peaks are visible in bulk PT, while the first four reflections are visible for the dispersions; nonetheless this is sufficient to identify the $Pn3m$ nanostructures and evaluate their lattice parameters. Peaks highlighted by asterisks indicate the co-existence of $Ia3d$ type cubic phase, which usually forms with lower water contents, and thus is not seen for dispersions. Lipid particles with 'cubic nanostructure' in their interior are commonly called as 'cubosomes'. **(B)** Size distribution of cubosomes prepared using various stabilizers as measured by static light scattering. [Please click here to view a larger version of this figure.](#)

The interactions between the CNTs and lipid particles were studied using Raman spectroscopy (**Figure 4**). The samples: CNTs, lipid and CNT-stabilized lipid particles were dehydrated, first using nitrogen gas and then by keeping them in a vacuum desiccator for about 20 min. The spectra were recorded using a Horiba Jobin-Yvon LabRAM HR800 spectrometer equipped with an Andor electromagnet charged coupled device (CCD) for light detection and a video camera to guide spectral collection. A 532 nm excitation line of Nd:YAG laser was utilized to collect spectra in the range 100–4,000 cm⁻¹ using a grating of 600 g mm⁻¹ blazed at 750 nm. 50X long working distance objective with a numerical aperture of 0.50 was used to acquire the spectra and the confocal hole was set at 100 μ m. Before the measurements, the instrument was calibrated to the 520.8 cm⁻¹ spectral line of silicon. All spectra were collected at RT (25 °C) by placing the sample on Calcium Fluoride slides. Spectra were acquired using the 532 nm laser and accumulated 5 times with 1% exposure for 10 sec. LabSpec 6 spectroscopy software suite used for pre-processing the raw data and immediate data interrogation.

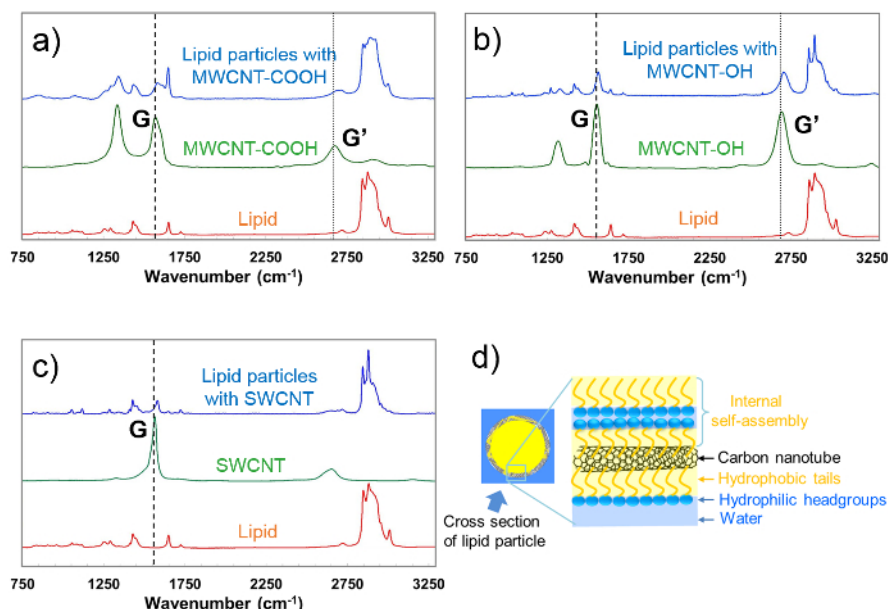


Figure 4. Raman spectra for dehydrated (A) pure lipid, MWCNT-COOH and CNT-stabilized lipid nanoparticles containing 5.0 µg/ml MWCNT-COOH, (B) pure lipid, MWCNT-OH and lipid nanoparticles containing 5.0 µg/ml MWCNT-OH, and (C) pure lipid, SWCNT and lipid nanoparticles containing 0.3125 µg/ml SWCNT. All curves represent an average of ten spectra where intensities, in arbitrary units are plotted versus wavelength. Vertical lines are used to guide the eye, and to ease the detection of the blue shifts in the G and G' bands. These experiments were performed for DU. (D) Schematic diagram of possible lipid decoration (self-assembling) on CNT surface (figure reproduced from reference [50] with permission from The Royal Society of Chemistry). [Please click here to view a larger version of this figure.](#)

Discussion

Stabilization of lipid particles

Three different CNTs are used to stabilize the lipid dispersions; two of which are multi-walled and functionalized using -OH and -COOH groups, and one is single walled and non-functionalized (pristine). The CNTs varied in size as follows (diameter x length): MWCNT-COOH: 9.5 nm x 1.5 µm; MWCNT-OH: 8-15 nm x 50 µm; SWCNT: 1-2 nm x 1-3 µm. The powdered CNTs were dispersed in water by probe ultra-sonication. Aforementioned sizes of CNTs are likely to decrease further due to ultra-sonication, albeit unevenly. CNT dispersions in pure water started separating after about 20 min, hence further work was executed within this time *i.e.*, addition of lipids and second sonication. The latter (ultrasonication performed on the lipid-CNT mixtures) assists in melting and breaking down large and inconsistent lipid domains formed during the hydration into sub-micron portions. Dispersing the bulk lipid in this manner facilitates the equilibrium formation of self-assembled nanostructures, which otherwise requires rigorous freeze-thaw cycles and/or long time (days to weeks). The bulk lipid phase breaks into nanoparticles whereas the lipid coated CNTs supposedly form shells around them. Ultra-sonication enhances the hydrophobic interactions between the CNTs and the alkyl chains of lipid molecules thereby decorating CNTs by lipid alkyl chains. Thus coated CNTs stabilize the fragmented lipid phase leading to a particulate emulsion. This mutual stabilization avoids the aggregation of CNTs as well as disperses the lipid particles. Such dispersions are also called Pickering (due to the use of solid particles) type oil-in-water (O/W) emulsions, where the lipids form an 'oil phase' while 'excess water' constitutes the continuous emulsion medium (Figure 1). Ultrasonication parameters (pulse length, delay time and power), physicochemical parameters of a stabilizer (*e.g.*, dimensions, functionalization), concentration of dispersed phase and composition of the dispersion (*e.g.*, CNT to lipid ratio) are crucial to guarantee the final stability of the dispersions and therefore need to be optimized for different (lipid) systems.

Optimization of CNT to lipid ratio for stable emulsions

A wide range of concentrations for each CNT-type (Figure 2) was employed to stabilize the self-assembled nanostructures obtained from two different lipids. However, homogeneous and stable emulsions are only formed in a particular range of CNT to lipid ratio; too high ratios cause aggregation of CNTs, while too low ratios lead to unstable emulsions, because there are not enough CNTs to accomplish a sufficient particle-surface coverage. Best stabilization conditions were found with concentrations between 3-5 µg/ml for MWCNT-COOH and MWCNT-OH, whereas for SWCNT in the range of 0.3-0.45 µg/ml.

Morphological characterization of lipid particles

The SAXS measurements verify that lipid particles of PT retain the original cubic phase nanostructure (shown by bulk phase) (Figure 3A). We presume that the cubic phase is also retained in case of DU particles, however this needs further confirmation as it was not studied in the current work. The lattice parameter observed for bulk *Pn3m* phase of PT is 6.84 nm, which upon dispersion increases to 7.1 nm. The lower lattice parameter for bulk phase is attributed to the lack of excess water, which can be also confirmed by the coexistence of *la3d* phase (peaks marked by * in Figure 3A). The *la3d* phase is usually found under limited water conditions. The lattice parameters for *Pn3m* phase observed for all dispersed lipid particles (*i.e.*, stabilized by surfactant as well as by all CNT types) are practically the same indicating excess water conditions. This also rules out the possibility of CNT-driven disturbances at the molecular level which, otherwise, could have triggered a change of the lipid phase.

The size distributions of the cubosomes are given by the volume-weighted distributions as shown in **Figure 3B**. Although the CNT-stabilized particles display a wide size distribution, majority of the particles exhibit sizes between 532-760 nm which are comparable to the size of surfactant stabilized lipid particles (674 nm).

Lipid coating of CNTs

For pure CNTs, typical Raman graphite bands are seen in the Raman spectra. The G band which corresponds to the in-plane vibration of 'C-C bond', the D band (not shown) which is due to the presence of disorder in carbon systems and the G' band which is attributed to the overtone of the D band⁷⁰ are clearly observed. Upon interaction of CNT with lipid and on formation of CNT-stabilized lipid particles (compare green and blue curves in **Figure 4**), a shift to higher wavenumbers (blue shift) is observed. The observed blue shift, could be due to: i) high pressure exerted on CNTs during ultrasonication resulting in their dispersion as opposed to a bundled state when pure^{70,71}, and/or ii) interactions between CNTs and lipid molecules via coating of CNTs by lipids (such blue shift has been reported previously by Douroumis *et al.*⁷² for lipid coated SWCNTs).

The decrease in relative intensities of CNT peaks and appearance of lipid signals (from red curves of pure lipid (**Figure 4**) further confirms the coating of CNTs by lipid molecules. This suggests that the hydrophobic interactions between CNTs and alkyl chains of lipid molecules decorate the CNT surface in such a way that hydrophilic head groups face aqueous regions thus stabilizing O/W emulsion, as shown by the schematic in **Figure 4D**.

We have demonstrated a smart and simple method of kinetically stabilizing the O/W type emulsion of nanostructured lipid particles using various CNTs. Very low concentrations (<10 µg/ml) of CNTs are adequate to stabilize the lipid nanoparticle dispersion, which is promising specifically for *in vivo* applications. Decoration of CNTs by lipid molecules is anticipated to minimize their toxicity while improving the biocompatibility. The prospect of loading functional molecules within the lipid self-assembly as well as on the CNT surface provide limitless potential to the CNT-stabilized lipid particles in the area of biomedical sciences especially in the context of combination therapies against major diseases⁷³.

Disclosures

We have nothing to disclose.

Acknowledgements

We would like to thank Dr. Matthew J. Baker, now at the University of Strathclyde, Glasgow for the support with Raman experiments and Mr. Nick Gaunt for his prior work of this project.

References

- Peer, D. *et al.* Nanocarriers as an emerging platform for cancer therapy. *Nature Nanotech.* **2**, 751-760 (2007).
- White, R. R., Sullenger, B. A., & Rusconi, C. P. Developing aptamers into therapeutics. *J. Clin. Invest.* **106**, 929-934 (2000).
- Itaka, K., Chung, U.-I., & Kataoka, K. Supramolecular nanocarrier for gene and siRNA delivery. *Nippon Rinsho Jpn. J. Clin. Med.* **64**, 253-257 (2006).
- Xu, S. *et al.* Development of pH-responsive core-shell nanocarriers for delivery of therapeutic and diagnostic agents. *Bioorg. Med. Chem. Lett.* **19**, 1030-1034 (2009).
- Soppimath, K. S., Tan, D. C. W., & Yang, Y. Y. pH-triggered thermally responsive polymer core-shell nanoparticles for drug delivery. *Adv. Mater.* **17**, 318-323 (2005).
- Hans, M., & Lowman, A. Biodegradable nanoparticles for drug delivery and targeting. *Curr. Opin. Solid State Mater. Sci.* **6**, 319-327 (2002).
- Petros, R. A., & DeSimone, J. M. Strategies in the design of nanoparticles for therapeutic applications. *Nat Rev Drug Discov.* **9**, 615-627 (2010).
- Torchilin, V. P. Multifunctional nanocarriers. *Adv Drug Deliver Rev.* **64**, 302-315 (2012).
- Shmeeda, H. *et al.* Delivery of zoledronic acid encapsulated in folate-targeted liposome results in potent in vitro cytotoxic activity on tumor cells. *J. Controlled Release.* **146**, 76-83 (2010).
- Xu, Z. *et al.* The performance of docetaxel-loaded solid lipid nanoparticles targeted to hepatocellular carcinoma. *Biomaterials.* **30**, 226-232 (2009).
- Rosenthal, E. *et al.* Phase IV study of liposomal daunorubicin (DaunoXome) in AIDS-related Kaposi sarcoma. *Am. J. Clin. Oncol.-Canc.* **25**, 57-59 (2002).
- Dong, Y. D., Larson, I., Bames, T. J., Prestidge, C. A., & Boyd, B. J. Adsorption of Nonlamellar Nanostructured Liquid-Crystalline Particles to Biorelevant Surfaces for Improved Delivery of Bioactive Compounds. *ACS Appl Mater Inter.* **3**, 1771-1780 (2011).
- Rizwan, S. B., Boyd, B. J., Rades, T., & Hook, S. Bicontinuous cubic liquid crystals as sustained delivery systems for peptides and proteins. *Expert Opin. Drug. Deliv.* **7**, 1133-1144 (2010).
- Yoo, H. S., & Park, T. G. Folate receptor targeted biodegradable polymeric doxorubicin micelles. *J. Controlled Release.* **96**, 273-283 (2004).
- Khandare, J. J. *et al.* Dendrimer versus linear conjugate: Influence of polymeric architecture on the delivery and anticancer effect of paclitaxel. *Bioconjug. Chem.* **17**, 1464-1472 (2006).
- Prabaharan, M., Grailer, J. J., Pilla, S., Steeber, D. A., & Gong, S. Gold nanoparticles with a monolayer of doxorubicin-conjugated amphiphilic block copolymer for tumor-targeted drug delivery. *Biomaterials.* **30**, 6065-6075 (2009).
- Khan, J. *et al.* Targeted anticancer prodrug with mesoporous silica nanoparticles as vehicles. *Nanotechnology.* **22** (2011).
- Bianco, A., & Prato, M. Can carbon nanotubes be considered useful tools for biological applications? *Adv. Mater.* **15**, 1765-1768 (2003).
- Kam, N. W. S., & Dai, H. J. Carbon nanotubes as intracellular protein transporters: Generality and biological functionality. *J. Am. Chem. Soc.* **127**, 6021-6026 (2005).
- Kulkarni, C. V. Lipid crystallization: from self-assembly to hierarchical and biological ordering. *Nanoscale.* **4**, 5779-5791 (2012).
- Yaghmur, A. *et al.* *Drug Formulations Based on Self-Assembled Liquid Crystalline Nanostructures*. CRC Press 341-360 (2014).

22. Kulkarni, C. V. in *Advances in Planar Lipid Bilayers and Liposomes*. Academic Press Vol. 12 237-272 (2010).
23. Landau, E. M., & Navarro, J. V. *Application: US Pat, US2001/0025791A1*. (2001).
24. Kulkarni, C., Belsare, N., & Lele, A. Studies on shrikhand rheology. *J. Food Eng.* **74**, 169-177 (2006).
25. Mezzenga, R., Schurtenberger, P., Burbidge, A., & Michel, M. Understanding foods as soft materials. *Nature Mater.* **4**, 729-740 (2005).
26. Ubbink, J., Burbidge, A., & Mezzenga, R. Food structure and functionality: a soft matter perspective. *Soft Matter*. **4**, 1569-1581 (2008).
27. Dong, Y.-D., Larson, I., Hanley, T., & Boyd, B. J. Bulk and dispersed aqueous phase behavior of phytantriol: effect of vitamin E acetate and F127 polymer on liquid crystal nanostructure. *Langmuir*. **22**, 9512-9518 (2006).
28. Yaghmur, A., & Glatter, O. Characterization and potential applications of nanostructured aqueous dispersions. *Adv. Colloid Interface Sci.* **147**, 333-342 (2009).
29. Pardeike, J., Hommoss, A., & Müller, R. H. Lipid nanoparticles (SLN, NLC) in cosmetic and pharmaceutical dermal products. *Int. J. Pharm.* **366**, 170-184 (2009).
30. Yaghmur, A., Rappolt, M., Østergaard, J., Larsen, C., & Larsen, S. W. Characterization of bupivacaine-loaded formulations based on liquid crystalline phases and microemulsions: the effect of lipid composition. *Langmuir*. **28**, 2881-2889 (2012).
31. Singh, H., Ye, A., & Horne, D. Structuring food emulsions in the gastrointestinal tract to modify lipid digestion. *Prog. Lipid Res.* **48**, 92-100 (2009).
32. Angelova, A., Angelov, B., Mutafchieva, R., Lesieur, S., & Couvreur, P. Self-Assembled Multicompartment Liquid Crystalline Lipid Carriers for Protein, Peptide, and Nucleic Acid Drug Delivery. *Accounts Chem. Res.* **44**, 147-156 (2011).
33. Clogston, J., & Caffrey, M. Controlling release from the lipidic cubic phase. Amino acids, peptides, proteins and nucleic acids. *J. Controlled Release*. **107**, 97-111 (2005).
34. Shah, J. C., Sadhale, Y., & Chilukuri, D. M. Cubic phase gels as drug delivery systems. *Adv. Drug Deliver. Rev.* **47**, 229-250 (2001).
35. Boyd, B. J., Whittaker, D. V., Khoo, S. M., & Davey, G. Lyotropic liquid crystalline phases formed from glycerate surfactants as sustained release drug delivery systems. *Int. J. Pharm.* **309**, 218-226 (2006).
36. Drummond, C. J., & Fong, C. Surfactant self-assembly objects as novel drug delivery vehicles. *Curr. Opin. Colloid Interface Sci.* **4**, 449-456 (1999).
37. Zhao, X. Y., Zhang, J., Zheng, L. Q., & Li, D. H. Studies of cubosomes as a sustained drug delivery system. *J. Dispersion Sci. Technol.* **25**, 795-799, (2004).
38. Malmsten, M. Phase transformations in self-assembly systems for drug delivery applications. *J. Dispersion Sci. Technol.* **28**, 63-72 (2007).
39. Sadhale, Y., & Shah, J. C. Stabilization of insulin against agitation-induced aggregation by the GMO cubic phase gel. *Int. J. Pharm.* **191**, 51-64 (1999).
40. Amar-Yuli, I., Azulay, D., Mishraki, T., Aserin, A., & Garti, N. The role of glycerol and phosphatidylcholine in solubilizing and enhancing insulin stability in reverse hexagonal mesophases. *J. Colloid Interface Sci.* **364**, 379-387 (2011).
41. Rappolt, M. in *Advances in planar lipid bilayers and liposomes*. Vol. 5 (ed Leitmannova Lui, A.) Elsevier Inc., Amsterdam 253-283 (2006).
42. Rappolt, M., Cacho-Nerin, F., Morello, C., & Yaghmur, A. How the chain configuration governs the packing of inverted micelles in the cubic Fd 3 m-phase. *Soft Matter*. **9**, 6291-6300 (2013).
43. Kulkarni, C. V., Wachter, W., Iglesias-Salto, G., Engelskirchen, S., & Ahualli, S. Monoolein: a magic lipid? *Phys. Chem. Chem. Phys.* **13**, 3004-3021 (2011).
44. Yaghmur, A., de Campo, L., Sagalowicz, L., Leser, M. E., & Glatter, O. Emulsified Microemulsions and Oil-Containing Liquid Crystalline Phases. *Langmuir*. **21**, 569-577 (2005).
45. Kulkarni, C. V., & Glatter, O. in *Self-Assembled Supramolecular Architectures: Lyotropic Liquid Crystals. Surface and Interfacial Chemistry*. (ed Nissim Garti) Ch. 6, John Wiley & Sons, Inc. (2012).
46. Salonen, A., Muller, F. O., & Glatter, O. Internally Self-Assembled Submicrometer Emulsions Stabilized by Spherical Nanocolloids: Finding the Free Nanoparticles in the Aqueous Continuous Phase. *Langmuir*. **26**, 7981-7987 (2010).
47. Guillot, S., Bergaya, F., de Azevedo, C., Warmont, F., & Tranchant, J. F. Internally structured pickering emulsions stabilized by clay mineral particles. *J. Colloid Interface Sci.* **333**, 563-569 (2009).
48. Muller, F., Salonen, A., & Glatter, O. Monoglyceride-based cubosomes stabilized by Laponite: Separating the effects of stabilizer, pH and temperature. *Colloids Surf., A*. **358**, 50-56 (2010).
49. Salonen, A., Muller, F. O., & Glatter, O. Dispersions of Internally Liquid Crystalline Systems Stabilized by Charged Disklike Particles as Pickering Emulsions: Basic Properties and Time-Resolved Behavior. *Langmuir*. **24**, 5306-5314 (2008).
50. Gaunt, N. P., Patil-Sen, Y., Baker, M. J., & Kulkarni, C. V. Carbon nanotubes for stabilization of nanostructured lipid particles. *Nanoscale*. **7**, 1090-1095 (2015).
51. Pickering, S. U. Emulsions. *J. Chem. Soc.* **91**, 2001 (1907).
52. Ramsden, W. Separation of Solids in the Surface-Layers of Solutions and 'Suspensions' (Observations on Surface-Membranes, Bubbles, Emulsions, and Mechanical Coagulation). -- Preliminary Account. *Proceedings of the Royal Society of London*. **72**, 156-164 (1903).
53. Lin, Y. *et al.* Advances toward bioapplications of carbon nanotubes. *J. Mater. Chem.* **14**, 527-541 (2004).
54. Saito, N. *et al.* Safe Clinical Use of Carbon Nanotubes as Innovative Biomaterials. *Chem. Rev.* **114**, 6040-6079 (2014).
55. Pulskamp, K., Diabate, S., & Krug, H. F. Carbon nanotubes show no sign of acute toxicity but induce intracellular reactive oxygen species in dependence on contaminants. *Toxicol. Lett.* **168**, 58-74 (2007).
56. Smart, S. K., Cassidy, A. I., Lu, G. Q., & Martin, D. J. The biocompatibility of carbon nanotubes. *Carbon*. **44**, 1034-1047 (2006).
57. Colvin, V. L. The potential environmental impact of engineered nanomaterials. *Nat. Biotechnol.* **21**, 1166-1170 (2003).
58. Firme, C. P., III & Bandaru, P. R. Toxicity issues in the application of carbon nanotubes to biological systems. *Nanomed-Nanotechnol.* **6**, 245-256 (2010).
59. Haddon, R. C. Carbon nanotubes. *Accounts Chem. Res.* **35**, 997-997 (2002).
60. Kapralov, A. A. *et al.* Adsorption of Surfactant Lipids by Single-Walled Carbon Nanotubes in Mouse Lung upon Pharyngeal Aspiration. *Acs Nano*. **6**, 4147-4156 (2012).
61. Wallace, E. J., & Mark, S. P. S. Carbon nanotube self-assembly with lipids and detergent: a molecular dynamics study. *Nanotechnology*. **20**, 045101 (2009).
62. George, R. B. *Chest medicine: essentials of pulmonary and critical care medicine*. Lippincott Williams & Wilkins (2005).
63. Monteiro-Riviere, N. A., Nemanich, R. J., Inman, A. O., Wang, Y. Y., & Riviere, J. E. Multi-walled carbon nanotube interactions with human epidermal keratinocytes. *Toxicol. Lett.* **155**, 377-384 (2005).

64. Shvedova, A. *et al.* Exposure to carbon nanotube material: assessment of nanotube cytotoxicity using human keratinocyte cells. *J. Toxicol. Env. Heal. A.* **66**, 1909-1926 (2003).
65. Jia, G. *et al.* Cytotoxicity of carbon nanomaterials: single-wall nanotube, multi-wall nanotube, and fullerene. *Environ. Sci. Technol.* **39**, 1378-1383 (2005).
66. Sato, Y. *et al.* Influence of length on cytotoxicity of multi-walled carbon nanotubes against human acute monocytic leukemia cell line THP-1 in vitro and subcutaneous tissue of rats in vivo. *Mol. BioSyst.* **1**, 176-182 (2005).
67. Bottini, M. *et al.* Multi-walled carbon nanotubes induce T lymphocyte apoptosis. *Toxicol. Lett.* **160**, 121-126 (2006).
68. Cui, D., Tian, F., Ozkan, C. S., Wang, M., & Gao, H. Effect of single wall carbon nanotubes on human HEK293 cells. *Toxicol. Lett.* **155**, 73-85 (2005).
69. Huang, T., Toraya, H., Blanton, T., & Wu, Y. X-ray powder diffraction analysis of silver behenate, a possible low-angle diffraction standard. *J. Appl. Crystallogr.* **26**, 180-184 (1993).
70. Bokobza, L., & Zhang, J. Raman spectroscopic characterization of multiwall carbon nanotubes and of composites. *Express Polym. Lett.* **6**, 601-608 (2012).
71. Zhao, Q., & Wagner, H. D. Raman spectroscopy of carbon-nanotube-based composites. *Philos. Trans. R. Soc. London, Ser. A -Math. Phys. Eng. Sci.* **362**, 2407-2424 (2004).
72. Douroumis, D., Fatouros, D. G., Bouropoulos, N., Papagelis, K., & Tasis, D. Colloidal stability of carbon nanotubes in an aqueous dispersion of phospholipid. *Int. J. Nanomed.* **2**, 761-766 (2007).
73. Worthington, R. J., & Melander, C. Combination approaches to combat multidrug-resistant bacteria. *Trends Biotechnol.* **31**, 177-184 (2013).